

Para-Derivatized Pybox Ligands As Sensitizers in Highly Luminescent Ln(III) Complexes

Ana de Bettencourt-Dias,^{*,†} Patrick S. Barber,[†] Subha Viswanathan,[‡] Daniel T. de Lill,[†] Alexandra Rollett,[‡] George Ling,[‡] and Sultan Altun[†]

[†]University of Nevada, Reno, Department of Chemistry, Reno, Nevada 89557, and [‡]Syracuse University, Department of Chemistry, Syracuse, New York 13244

Received May 21, 2010

New complexes of pyridine-bis(oxazoline) derivatized with -H, -OMe, and -Br at the para position of the pyridine ring with Eu(III) and Tb(III) have been isolated. These are highly luminescent in the solid state, regardless of the ligand-to-metal ratio. Several of the metal complexes were isolated and characterized by single crystal X-ray diffraction, showing the rich diversity of structures that can be obtained with this family of ligands. [Eu(PyboxOMe)₃](NO₃)₃·3CH₂Cl₂, **1**, crystallizes in the monoclinic space group *P*2₁/*n* and has the cell parameters *a* = 14.3699(10) Å, *b* = 13.4059(9) Å, *c* = 25.8766(18) Å, β = 95.367(1)°, and *V* = 4963.1(6) Å³. The isostructural [Tb(PyboxOMe)₃](NO₃)₃·3CH₂Cl₂, **2**, crystallizes with the parameters *a* = 14.4845(16) Å, *b* = 13.2998(15) Å, *c* = 25.890(3) Å, β = 94.918(2)°, and *V* = 4969.1(10) Å³. **3**, a 1:1 complex with the formula [Eu(PyboxBr)(NO₃)₃(H₂O)], crystallizes in the monoclinic *P*2₁/*c* space group with *a* = 11.649(2) Å, *b* = 8.3914(17) Å, *c* = 20.320(4) Å, β = 100.25(3)°, and *V* = 1954.5(7) Å³. **4**, a product of the reaction of PyboxBr with Tb(NO₃)₃, is [Tb(PyboxBr)₂(η^2 -NO₃)(η^1 -NO₃)₂][Tb(NO₃)₅]·5H₂O. It crystallizes in the monoclinic space group *P*2₁ with *a* = 15.612(3) Å, *b* = 14.330(3) Å, *c* = 16.271(3) Å, β = 92.58(3)°, and *V* = 3636.5(13) Å³. [Tb(Pybox)₃](CF₃SO₃)₃·3CH₂CN, **5**, crystallizes in the triclinic space group *P* $\bar{1}$ with *a* = 12.3478(2) Å, *b* = 15.0017(2) Å, *c* = 16.1476(4) Å, α = 100.252(1)°, β = 100.943(1)°, γ = 113.049(1)°, and *V* = 2594.80(8) Å³. Finally, compound **6**, [Tb(Pybox)₂(NO₃)(H₂O)](NO₃)₂·CH₃OH, crystallizes in the triclinic *P* $\bar{1}$ space group with *a* = 9.7791(2) Å, *b* = 10.1722(2) Å, *c* = 15.3368(3) Å, α = 83.753(1)°, β = 78.307(1)°, γ = 85.630(1)°, and *V* = 1482.33(5) Å³. In solution, the existence of 3:1, 2:1, and 1:1 species can be observed through absorption and luminescence speciation measurements as well as NMR spectroscopy. The stability constants in acetonitrile, as an average obtained from absorption and emission titrations, are log β_{11} = 5.4, log β_{12} = 8.8, and log β_{13} = 12.8 with Eu(III) and log β_{11} = 4.5, log β_{12} = 8.4, and log β_{13} = 11.7 for the Tb(III) species with PyboxOMe. Pybox displayed stability constants log β_{11} = 3.6, log β_{12} = 9.1, and log β_{13} = 12.0 with Eu(III) and log β_{11} = 3.7, log β_{12} = 9.3, and log β_{13} = 12.2 for the Tb(III) species. Finally, PyboxBr yielded log β_{11} = 7.1, log β_{12} = 12.2, and log β_{13} = 15.5 for the Eu(III) species and log β_{11} = 6.2, log β_{12} = 11.0, and log β_{13} = 15.4 with Tb(III). Photophysical characterization was performed in all cases on solutions with 3:1 ligand-to-metal ion stoichiometry and allowed determination of quantum yields and lifetimes of emission for PyboxOMe of 23.5 ± 1.6% and 1.54 ± 0.04 ms for Eu(III) and 21.4 ± 3.6% and 1.88 ± 0.04 ms for Tb(III). For Pybox these values were 25.6 ± 1.1% and 1.49 ± 0.04 ms for Eu(III) and 23.2 ± 2.1% and 0.44 ± 0.01 ms for Tb(III) and for PyboxBr they were 35.8 ± 1.6% and 1.46 ± 0.03 ms for Eu(III) and 23.3 ± 1.3% and a double lifetime of 0.79 ± 0.05/0.07 ± 0.01 ms for Tb(III). A linear relationship between the triplet level energies and the Hammett σ constants was found. Lifetime measurements in methanol as well as the NMR data in both methanol and acetonitrile indicate that all complexes are stable in the 3:1 stoichiometry in solution and that there is no solvent coordination to the metal ion.

Introduction

The luminescence of lanthanide ion (Ln(III)) complexes is a well-known phenomenon. The f-f transitions, which are responsible for the light emission, are narrow and characteristic of each ion, and the emitting excited states are long-lived.

These properties make Ln(III) ion emission suitable for applications ranging from phosphors for lighting and display applications to biosensing and fluoroimmunoassays.^{1–3} One

*To whom correspondence should be addressed. E-mail: abd@unr.edu.
Phone: 775 682 8421. Fax: 775 784 6804.

(1) de Bettencourt-Dias, A. *Dalton Trans.* 2007, 2229–2241.
(2) Bünzli, J.-C. G. Rare earth luminescent centers in organic and biochemical compounds. In *Spectroscopic Properties of Rare Earths in Optical Materials*; Liu, G., Jacquier, B., Eds.; Springer: Berlin, 2005; Vol. 83, pp 462–499.

limitation for the applicability of the Ln(III) ions is the fact that f-f transitions are spin and parity forbidden. To overcome this limitation organic ligands are utilized as sensitizers. In the sensitization process the ligand absorbs energy and transfers it to the metal ion, through successive population of ligand-based singlet and triplet states and a final energy transfer step to the emissive state on the Ln(III) ion.^{2,4} Several different types of sensitizers have been reported and have been recently reviewed.^{4–13} An organic ligand which had not been tested as a sensitizer until recently is pyridine-bis(oxazoline) (Pybox). Pybox derivatives have found widespread use as ligands for asymmetric transition metal catalysts.¹⁴ More recently, Aspinall and co-workers utilized this type of ligand in enantioselective synthesis with lanthanide ion based catalysts.^{15–18} This ligand moiety displays aromaticity and good electronic absorption properties. Further, it is tridentate, potentially yielding stable compounds and derivatives with functional groups both at the oxazoline as well as the para-position of the pyridine ring are known.^{14,19} In a previous publication our group described highly luminescent Eu(III) and Tb(III) complexes of Pybox derivatized with thiophen-3-yl at the para position of the pyridine ring, PyboxTh.²⁰ A 2:1 ligand-to-metal ion complex was isolated in the solid state, and solution speciation experiments pointed to the additional formation of the 1:1 and 3:1 species. The quantum yields of luminescence for the complexes in solution with the 3:1 stoichiometry were 76.2% for Eu(III) and 58.6% for Tb(III), indicating, especially in the case of the former metal ion, an excellent energy match between the triplet state energy of the ligand and the emissive state of Eu(III). We became therefore interested in the Pybox moiety as a chelator and sensitizer of Ln(III) ions, with its potential for further derivatization and thus tuning of the ligand energy levels. In initial studies we utilized thiophen-3-yl, a moderate electron-donating group in the para position of the pyridine ring. We also explored oxazoline-derivatized Pybox ligands, which displayed good luminescence characteristics

but because of the steric nature of the oxazoline substituents form at most the 2:1 species and thus do not saturate the coordination sphere of the lanthanide ion with ligands.²¹ Similar 2:1 species with oxazoline-derivatized Pybox ligands were communicated recently also by Matsumoto et al.²² After the PyboxTh moiety, we subsequently set out to use on the para position of the pyridine ring a more strongly electron-donating moiety, methoxy, as well as bromo, an electron-withdrawing moiety. Here we describe synthesis of the methoxy and bromo-derivatized Pybox (PyboxOMe and PyboxBr, respectively) and of their complexes with Eu(III) and Tb(III). These two ligands were previously unknown. For comparison, the underivatized Pybox, recently described as a chelator for Cu(I) in catalysis²³ and as a La(III) complex based ionization probe for mass spectrometry,²⁴ and its lanthanide ion complexes were also studied. The solid state structures of several complexes of these ligands are discussed. All isolated crystals are luminescent, and the emission efficiency was quantified in solution for the 3:1 ligand-to-metal ion species. The results obtained confirm the initial hypothesis that the Pybox moiety is a good sensitizer of Ln(III) ion luminescence, as the triplet and singlet states of the three ligands studied here are adequately located. Further, this type of ligand coordinates strongly to the Ln(III) ions in solution, saturating the coordination sphere of the metal ion in the 3:1 stoichiometry and preventing thus solvent-induced quenching of the luminescence. Finally, despite the fact that in some cases lanthanide salts with the coordinating nitrate counterion were utilized,²⁵ the Pybox-based ligands rapidly displaces the nitrate, and isolation of the metal ion complexes in all possible ligand-to-metal ion stoichiometries is easily accomplished. Since the 3:1 stoichiometry is stable, no effect of the lanthanide salt counterion on the photophysical properties was observed.

Experimental Section

All commercially obtained reagents were of analytical grade and used as received. Solvents were dried by standard methods.²⁶ Lanthanide salts were dried under reduced pressure and heating and kept in a glovebox under controlled atmosphere ($O_2 < 0.2$ ppm, $H_2O < 5$ ppm). Unless otherwise indicated, all data were collected at a constant temperature of 25.0 ± 0.1 °C.

NMR spectra were recorded on a Bruker Avance DPX 300 or on Varian 400 and 500 spectrometers with chemical shifts reported (δ , ppm) against tetramethylsilane (SiMe₄). The metal complex solutions were prepared by mixing appropriate amounts of ligand and Ln(III) salt (Ln = La or Lu) in 3:1 stoichiometry. Absorption spectra were obtained on a Perkin-Elmer Lambda 35 spectrometer. Fluorescence spectra were obtained on a Perkin-Elmer LS-55 spectrometer.

Electrospray ionization mass spectra (ESI-MS) were collected in positive ion mode on a Waters Micromass ZQ quadrupole mass spectrometer. The samples were prepared by diluting the solutions utilized for NMR spectroscopy to a

(3) Bünzli, J.-C. G.; Choppin, G. R. *Lanthanide Probes in Life, Chemical and Earth Sciences - Theory and Practice*; Elsevier: Amsterdam, The Netherlands, 1989.

(4) de Bettencourt-Dias, A. *Curr. Org. Chem.* **2007**, *11*, 1460–1480.

(5) Katkova, M. A.; Bochkarev, M. N. *Dalton Trans.* **2010**, *39*, 6599–6612.

(6) Bünzli, J.-C. G. *Chem. Rev.* **2010**, *110*, 2729–2755.

(7) Eliseeva, S. V.; Bünzli, J.-C. G. *Chem. Soc. Rev.* **2010**, *39*, 189–227.

(8) dos Santos, C. M. G.; Harte, A. J.; Quinn, S. J.; Gunnlaugsson, T. *Coord. Chem. Rev.* **2008**, *252*, 2512–2527.

(9) New, E. J.; Parker, D.; Smith, D. G.; Walton, J. W. *Curr. Opin. Chem. Biol.* **2010**, *14*, 238–246.

(10) Montgomery, C. P.; Murray, B. S.; New, E. J.; Pal, R.; Parker, D. *Acc. Chem. Res.* **2009**, *42*, 925–937.

(11) Allain, C.; Faulkner, S. *Future Med. Chem.* **2010**, *2*, 339–350.

(12) Faulkner, S.; Natrajan, L. S.; Perry, W. S.; Sykes, D. *Dalton Trans.* **2009**, 3890–3899.

(13) Faulkner, S.; Pope, S. J. A.; Burton-Pye, B. P. *Appl. Spectrosc. Rev.* **2005**, *40*, 1–31.

(14) Desimoni, G.; Faita, G.; Quadrelli, P. *Chem. Rev.* **2003**, *103*, 3119–3154.

(15) Aspinall, H. C. *Chem. Rev.* **2002**, *102*, 1807–1850.

(16) Aspinall, H. C.; Bickley, J. F.; Greeves, N.; Kelly, R. V.; Smith, P. M. *Organometallics* **2005**, *24*, 3458–3467.

(17) Aspinall, H. C.; Dwyer, J. L. M.; Greeves, N.; Smith, P. M. *J. Alloys Compd.* **2000**, *303–304*, 173–177.

(18) Aspinall, H. C.; Greeves, N. *J. Organomet. Chem.* **2002**, *647*, 151–157.

(19) Desimoni, G.; Faita, G.; Jorgensen, K. A. *Chem. Rev.* **2006**, *106*, 3561–3651.

(20) de Bettencourt-Dias, A.; Viswanathan, S.; Rollett, A. J. *Am. Chem. Soc.* **2007**, *129*, 15436–15437.

(21) de Bettencourt-Dias, A.; Barber, P. S. C. *R. Chim.* **2010**, *13*, 691–699.

(22) Matsumoto, K.; Suzuki, K.; Tsukuda, T.; Tsubomura, T. *Inorg. Chem.* **2010**, *49*, 4717–4719.

(23) Liang, Y.; Zhou, H.; Yu, Z.-X. *J. Am. Chem. Soc.* **2009**, *131*, 17783–17785.

(24) Ito, F.; Nakamura, T.; Yorita, S.; Danjo, H.; Yamaguchi, K. *Tetrahedron Lett.* **2009**, *50*, 6252–6255.

(25) Escande, A.; Guéneé, L.; Buchwalder, K.-L.; Piguet, C. *Inorg. Chem.* **2009**, *48*, 1132–1147.

(26) Pangborn, A. B.; Giardello, M. A.; Grubbs, R. H.; Kosen, R. K.; Timmers, F. J. *Organometallics* **1996**, *15*, 1518–1520.

concentration of ~ 1 mg/mL with acetonitrile. All samples were filtered through a $0.2 \mu\text{m}$ syringe filter before injecting into the mass spectrometer.

Elemental analyses were performed at Galbraith Laboratories (Knoxville, TN).

Ligand Synthesis. All three ligands were synthesized in a similar way to the previously reported thiophen-3-yl derivative of pyridine-bis(oxazoline)²⁰ and according to modified literature procedures.²⁷

Synthesis of Pybox. Dipicolinic acid (2.60 g, 15.4 mmol) was treated with PBr_5 at $85\text{--}90^\circ\text{C}$ for 5 h. The reaction residue was cooled and extracted three times with chloroform and evaporated to yield the acid bromide of dipicolinic acid. The CHCl_3 solution of the acid bromide was added to an aqueous solution of chloroethylamine hydrochloride (3.93 g, 33.9 mmol) and KOH (2.59 g, 46.2 mmol) at 0°C . The resulting solution was stirred at 0°C . After 50 min the aqueous layer was separated, the organic layer filtered, washed with water, and the solvent removed under reduced pressure to yield the crude carboxamide as a white powder. This white powder was dissolved in tetrahydrofuran (THF) and added to a suspension of NaH (2 g, 60% in mineral oil) in THF at 0°C . The reaction mixture was stirred at room temperature for 24 h, after which it was quenched with 10% HCl. The THF was removed under reduced pressure, the residue dissolved in dichloromethane, washed with brine, and dried over MgSO_4 . After removal of the solvent under reduced pressure, the product was isolated as a white powder in 43% overall yield from dipicolinic acid. $^1\text{H NMR}$ (400 MHz, CDCl_3 , TMS) δ 8.14 (d, 2H, $^3J = 7.8$ Hz), 7.95 (t, $^3J = 7.9$ Hz, 1H), 4.50 (t, $^3J = 9.5$ Hz, 4H), 4.06 (t, $^3J = 7.8$ Hz, 4H). $^{13}\text{C NMR}$ (101 MHz, CDCl_3 , TMS) δ 163.48, 146.76, 137.40, 125.53, 68.37, 55.08. ESI-MS(+): m/z : 218.09 [HPybox]⁺ (calcd 218.23). Anal. Calculated for Pybox $\cdot 0.5$ ethanol: C, 59.99; H, 5.87; N, 17.49. Found: C, 60.08; H, 5.52; N, 17.82.

Synthesis of PyboxOMe. Chelidamic acid (4.66 g, 25 mmol) was treated with PBr_5 at 85°C for 6 h to yield the acid bromide. Addition of the acid bromide in CHCl_3 to an aqueous solution of chloroethylamine hydrochloride (6.38 g, 55 mmol) and KOH (6.16 g, 111 mmol) at 0°C led to the formation of the carboxamide intermediate. The carboxamide was purified by separation of the organic layer, washing with sat. NaHCO_3 , drying of the organic layer with MgSO_4 , and removal of the organic solvent under reduced pressure. The carboxamide was then treated with an excess of KOH in methanol and refluxed overnight. Addition of water to the cooled reaction mixture led to the formation of the product as a white precipitate. Filtration and drying under reduced pressure afforded the desired product in 36% overall yield from chelidamic acid. $^1\text{H NMR}$ (400 MHz, CDCl_3 , TMS) δ 7.69 (s, 2H), 4.53 (t, $^3J = 9.7$ Hz, 4H), 4.11 (t, $^3J = 9.7$ Hz, 4H), 3.94 (s, 3H). $^{13}\text{C NMR}$ (101 MHz, CDCl_3 , TMS) δ 166.59, 163.58, 148.28, 111.61, 68.35, 55.84, 55.02. ESI-MS(+): m/z : 248.00 [HPyboxOMe]⁺ (calcd 248.26). Anal. Calculated for PyboxOMe $\cdot 0.5$ methanol: C, 57.03; H, 5.74; N, 15.96. Found: C, 57.08; H, 5.58; N, 16.08.

Synthesis of PyboxBr. Chelidamic acid (3.33 g, 14 mmol) was treated with PBr_5 at $85\text{--}90^\circ\text{C}$ for 5 h. The residue was cooled to room temperature, and extracted three times with CHCl_3 . The chloroform was removed under reduced pressure to yield the acid bromide of chelidamic acid. To the crude acid bromide, chloroethylamine hydrochloride (3.45 g, 30 mmol), and KOH (3.36 g, 60 mmol) were added in water at 0°C and stirring for 50 min. After separation of the organic layer, filtration, washing with water and removal of the organic solvent under reduced pressure, the carboxamide intermediate was obtained as a white powder. The amide was dissolved in THF and added to a suspension of NaH (3.5 g, 60% in mineral oil) at 0°C . The reaction

mixture was subsequently stirred at room temperature for 20 h and quenched with 10% HCl. THF was removed under reduced pressure, dichloromethane was added, and the solution was washed with brine, dried over MgSO_4 , and the solvent was removed under reduced pressure. The white residue was recrystallized from ethanol to provide the desired compound as a white crystalline solid in 18% overall yield from chelidamic acid. $^1\text{H NMR}$ (400 MHz, CDCl_3 , TMS) δ 8.30 (s, 2H), 4.48 (t, $^3J = 9.8$ Hz, 4H), 4.05 (t, $^3J = 9.7$ Hz, 4H). $^{13}\text{C NMR}$ (101 MHz, CDCl_3 , TMS) δ 162.48, 147.60, 133.76, 128.66, 68.54, 55.03. ESI-MS(+): m/z : 295.99, 298.01 [HPyboxBr]⁺ (calcd 296.00, 298.00). Anal. Calculated for PyboxBr $\cdot 0.5$ ethanol: C, 45.16; H, 4.11; N, 13.17. Found: C, 45.66; H, 3.79; N, 13.38.

Synthesis of Metal Complexes. All metal complexes were prepared in a similar manner in air by mixing stoichiometric amounts of ligand and $\text{Ln}(\text{NO}_3)_3$ or $\text{Ln}(\text{CF}_3\text{SO}_3)_3$ ($\text{Ln} = \text{Eu}, \text{Tb}$) in acetonitrile. After refluxing for 1 h, the solvent was removed under reduced pressure, and a minimum amount of acetonitrile, dichloromethane, or methanol was added to form a saturated solution. The solution was filtered, and slow solvent evaporation yielded X-ray quality single crystals within a few days. Since only crystallization was attempted and bulk solids were not routinely isolated from the solution, yields were not determined.

For the 3:1 ligand-to-metal ion species the following were obtained:

PyboxOMe

$\text{Ln} = \text{Eu}$: ESI-MS(+): m/z : 297.82 [$\text{Eu}(\text{PyboxOMe})_3$]³⁺ (calcd 297.90)

$\text{Ln} = \text{Tb}$: ESI-MS(+): m/z : 300.38 [$\text{Tb}(\text{PyboxOMe})_3$]³⁺ (calcd 300.23)

PyboxBr

$\text{Ln} = \text{Eu}$: ESI-MS(+): m/z : 346.75 [$\text{Eu}(\text{PyboxBr})_3$]³⁺ (calcd 346.75)

$\text{Ln} = \text{Tb}$: ESI-MS(+): m/z : 349.14 [$\text{Tb}(\text{PyboxBr})_3$]³⁺ (calcd 349.08)

Pybox

$\text{Ln} = \text{Eu}$: ESI-MS(+): m/z : 267.74 [$\text{Eu}(\text{Pybox})_3$]³⁺ (calcd 267.88)

$\text{Ln} = \text{Tb}$: ESI-MS(+): m/z : 270.18 [$\text{Tb}(\text{Pybox})_3$]³⁺ (calcd 270.20)

X-ray Crystallographic Characterization. Crystal data, data collection, and refinement details for compounds 1–6 are given in Table 1. Selected bond lengths and angles for these complexes as well as selected hydrogen bond distances are given in the Supporting Information, Tables S1–S10. Suitable crystals were mounted on a glass fiber and placed in the low-temperature nitrogen stream. Data were collected on a Bruker SMART CCD area detector diffractometer equipped with a low-temperature device, using graphite-monochromated Mo-K α radiation ($\lambda = 0.71073 \text{ \AA}$). Data were measured using a strategy combining ω and φ scans of 0.3° per frame and an acquisition time of 10 or 20 s per frame. Multiscan absorption corrections were applied. Cell parameters were retrieved using the SMART²⁸ software and refined using SAINTPlus²⁹ on all observed reflections. Data reduction and correction for Lp and decay were performed using the SAINTPlus²⁹ software. Absorption corrections were applied using SADABS.³⁰ The structures were solved by direct methods and refined by least-squares methods on F^2 using the SHELXTL³¹ program package. All non-hydrogen atoms were refined anisotropically. The hydrogen atoms were added geometrically, and their parameters constrained to the parent site.

(28) SMART, Bruker Molecular Analysis Research Tool, v.5.626; Bruker AXS: Madison, WI, 2002.

(29) SAINTPlus, Data Reduction and Correction Program, v.6.36a; Bruker AXS: Madison, WI, 2001.

(30) SADABS, an empirical absorption correction program, v.2.01; Bruker AXS: Madison, WI, 2001.

(31) Sheldrick, G. M. SHELXTL, Structure Determination Software Suite, v.6.10; Bruker AXS: Madison, WI, 2001.

(27) Nishiyama, H.; Sakaguchi, H.; Nakamura, T.; Horihata, M.; Kondo, M.; Itoh, K. *Organometallics* **1989**, *8*, 846–848.

Table 1. Details of the X-ray Crystallographic Characterization of Compounds 1–6

complex	1	2	3	4	5	6
CCDC no.	746871	746872	755121	755122	755120	755119
formula	C ₇₇ H ₈₈ Cl ₁₀ Eu ₂ ·N ₂₄ O ₃₆	C ₇₇ H ₈₈ Cl ₁₀ N ₂₄ ·O ₃₆ Tb ₂	C ₁₁ H ₁₂ BrEu·N ₆ O ₁₂	C ₂₂ H ₂₅ Br ₂ N _{10.5} ·O ₂₀ Tb _{1.5}	C ₄₂ H ₄₂ F ₉ N ₁₂ ·O ₁₅ S ₃ Tb	C ₂₃ H ₂₆ N ₉ ·O ₁₅ Tb
M/g mol ⁻¹	2584.13	2598.05	652.14	1154.72	1380.98	827.45
crystal system	monoclinic	monoclinic	monoclinic	monoclinic	triclinic	triclinic
space group	<i>P</i> 2 ₁ / <i>n</i>	<i>P</i> 2 ₁ / <i>n</i>	<i>P</i> 2 ₁ / <i>c</i>	<i>P</i> 2 ₁	<i>P</i> $\bar{1}$	<i>P</i> $\bar{1}$
<i>a</i> /Å	14.3699(10)	14.4845(16)	11.649(2)	15.612(3)	12.3478(2)	9.7791(2)
<i>b</i> /Å	13.4059(9)	13.2998(15)	8.3914(17)	14.330(3)	15.0017(2)	10.1722(2)
<i>c</i> /Å	25.8766(18)	25.890(3)	20.320(4)	16.271(3)	16.1476(4)	15.3368(3)
α /deg	90	90	90	90	100.252(1)	83.753(1)
β /deg	95.367(1)	94.918(2)	100.25(3)	92.58(3)	100.943(1)	78.307(1)
γ /deg	90	90	90	90	113.049(1)	85.630(1)
<i>V</i> /Å ³	4963.1(6)	4969.1(10)	1954.5(7)	3636.5(13)	2594.80(8)	1482.33(5)
<i>T</i> /K	100(2)	100(2)	96(2)	95(2)	100(2)	99(2)
<i>Z</i>	2	2	4	4	2	2
<i>D_c</i> /g cm ⁻³	1.729	1.736	2.216	2.109	1.768	1.854
μ (Mo-K α)/mm ⁻¹	1.618	1.777	5.329	5.194	1.595	2.475
independent reflections, <i>R</i> _{int} [<i>F</i> _o ≥ 4 σ (<i>F</i> _o)]	1461, 0.0525	14482, 0.0363	4813, 0.0422	17842, 0.0497	15016, 0.0215	8570, 0.0286
reflections collected	65992	57457	20654	38786	83135	46351
<i>R</i> ₁ , <i>wR</i> ₂ [<i>I</i> > 2 σ (<i>I</i>)]	0.0471, 0.0992	0.0411, 0.0979	0.0385, 0.1088	0.0625, 0.1472	0.0207, 0.0562	0.0332, 0.0857
data/restraints/parameters	14461/2/679	14482/2/679	4813/0/288	17842/63/1010	15016/0/742	8570/6/435
GoF on <i>F</i> ²	1.071	1.024	1.046	1.027	1.126	1.222
largest diff. peak and hole/e Å ⁻³	2.243, -2.219	3.190, -3.249	2.581, -2.512	3.792, -3.722	1.379, -0.761	3.204, -1.697

For complexes with coordinated water molecules and water molecules of crystallization, their hydrogen atoms could not be located on the difference map, could not be added geometrically, and have been omitted, although the formulas are correct. X-ray crystallographic information files can either be found on the same Web site or can be obtained free of charge via www.ccdc.cam.ac.uk/conts/retrieving.html (or from the CCDC, 12 Union Road, Cambridge CB2 1EZ, U.K.; fax +44 1223 336033; e-mail data_request@ccdc.cam.ac.uk). CCDC 746871 contains the supplementary crystallographic data for **1**, CCDC 746872 for **2**, CCDC 755121 for **3**, CCDC 755122 for **4**, CCDC 755120 for **5**, and CCDC 755119 for **6** in this paper.

Determination of Stability Constants. All the solutions were prepared in a glovebox with controlled atmosphere ($O_2 < 0.2$ ppm, $H_2O < 5$ ppm) in analytical grade acetonitrile at constant ionic strength, *I* = 0.1 M, using Et₄NCl. Stock solutions of lanthanide ions at 0.01 M were prepared by dissolving appropriate quantities of dry Ln(CF₃SO₃)₃ or Ln(NO₃)₃ (Ln = Eu, Tb) in analytical grade dry acetonitrile. The concentration of metal ion the hexamine buffered solutions was determined by titration with standardized ethylenediaminetetraacetic acid (EDTA) (0.01 M) using xylenol orange as indicator.³² The stock solutions of the three ligands were also prepared at 0.01 M concentration in dry acetonitrile and were diluted as needed.

In a typical experiment 25 mL of 1 × 10⁻⁴ M ligand was titrated against metal salt solution, under argon. After each addition of the metal ion and a delay of 5 min, the absorption or emission spectrum was measured. Each titration run had at least 30 data points to allow for a good fitting. It was also ensured that a wide range of ligand-to-metal ion stoichiometric ratios was considered. Three repeat titrations were performed for each system to account for experimental errors. Refinement of stability constants was performed using the HYPERQUAD2006³³ software package.

Photophysical Characterization. Solutions for spectroscopic studies were prepared by mixing the ligands with lanthanide nitrates or triflates in acetonitrile in 3:1 stoichiometry in a glovebox with controlled atmosphere ($O_2 < 0.2$ ppm, $H_2O < 5$ ppm). The formed solutions were diluted to an approximate final concentration of 10⁻⁴ M and allowed to equilibrate in the

glovebox prior to measurement. The final metal ion concentration was determined by titration with EDTA with xylenol orange as the indicator.³² Absorption spectra were measured on a Perkin-Elmer Lambda 35 spectrometer and emission spectra on a Perkin-Elmer LS-55 fluorescence spectrometer in air, since comparison emission data collected under argon reveal no difference in the obtained data. Slit widths for emission and excitation measurements were 5 and/or 10 nm and a scan rate of 250 nm/sec was used. The data were collected in phosphorescence mode with a delay of 0 ms, a cycle time of 16 ms and a gate time of 0.05 ms. The solutions for all the photophysical measurements were allowed to equilibrate for 2 to 3 h before being used. For quantum yield measurements, both the absorption and the emission/excitation spectra were measured using 0.2 cm path length cells, making sure that while measuring the spectra the emitted light is at right angle and along the long path length (1 cm). All measurements, except the triplet-state measurements, were performed at 25.0 ± 0.1 °C. The triplet-state measurements were performed at 77 K, as described by Crosby.³⁴ Quantum yields were calculated using the equation below.

$$\Phi_x = \frac{n_x^2 A_{ref} I_{ref} E_x}{n_{ref}^2 A_x I_x E_{ref}} \times \Phi_{ref}$$

Φ is the quantum yield of sample *x* and reference *ref*, *n* is the refractive index (1.343 in acetonitrile, 1.33287 in water), *A* the absorbance at the excitation wavelength, *I* the intensity of the corrected excitation spectrum at the excitation wavelength, and *E* the integrated corrected emission spectrum. The spectra are always corrected for instrumental functions. Quantum yields for the reported solutions were measured against Cs₃[Eu(dipic)₃] ($\Phi_{ref} = 24.0\%$, $A_{279} \approx 0.15$, 7.5×10^{-5} M) and Cs₃[Tb(dipic)₃] ($\Phi_{ref} = 22.0\%$, $A_{279} \approx 0.15$, 6.5×10^{-5} M) in Tris buffer (0.1 M) as reference.^{35,36} The excitation wavelengths of the samples were chosen to ensure that there is a linear relationship between the intensity of emitted light and the concentration of the absorbing/emitting species (*A* ≤ 0.05).

All reported data are the average of at least three independent measurements.

(34) Crosby, G. A.; Whan, R. E.; Alire, R. M. *J. Chem. Phys.* **1961**, *34*, 743–748.

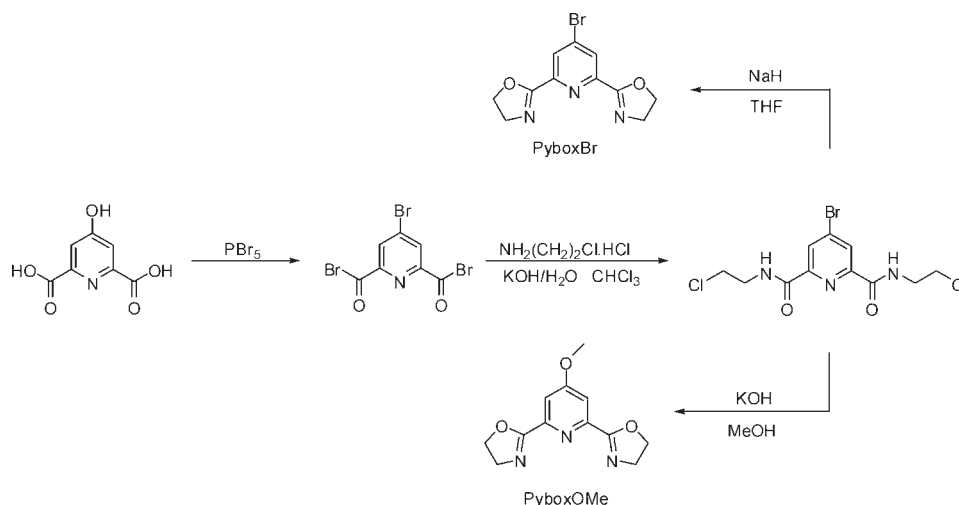
(35) Chauvin, A.-S.; Gumy, F.; Imbert, D.; Bünzli, J.-C. G. *Spectrosc. Lett.* **2004**, *37*, 517–532.

(36) Chauvin, A.-S.; Gumy, F.; Imbert, D.; Bünzli, J.-C. G. *Spectrosc. Lett.* **2007**, *40*, 193.

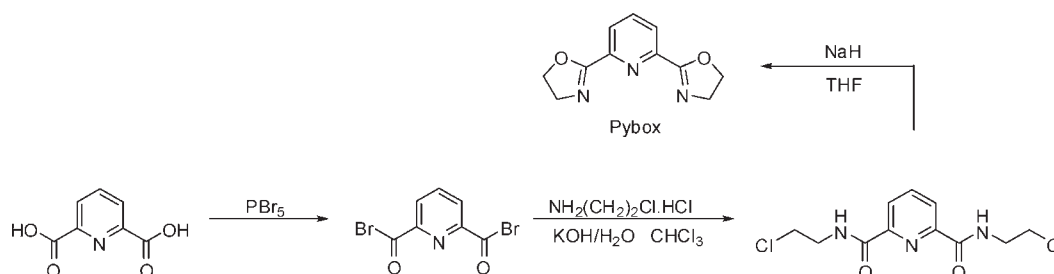
(32) Bassett, J.; Denney, R. C.; Jeffery, G. H.; Mendham, J. *Vogel's Textbook of Quantitative Inorganic Analysis*, 4th ed.; Longman Group Ltd.: London, U.K., 1978.

(33) Gans, P.; Sabatini, A.; Vacca, A. *Talanta* **1996**, *43*, 1739–1753.

Scheme 1. Synthesis of PyboxOMe and PyboxBr



Scheme 2. Synthesis of Pybox



Results and Discussion

Three ligands of para-derivatized pyridine-bis(oxazoline), Pybox, were synthesized and characterized: methoxy-derivatized Pybox (PyboxOMe), bromo-derivatized Pybox (PyboxBr), both of which were unknown, and Pybox. X-ray quality crystals of several complexes of $\text{Eu}(\text{III})$ and $\text{Tb}(\text{III})$ with these ligands were isolated. When examined under the light of a hand-held UV lamp ($\lambda = 245 \text{ nm}$), the crystals display the characteristic red or green luminescence of the corresponding lanthanide ion. Solutions of the ligands with $\text{Eu}(\text{III})$ and $\text{Tb}(\text{III})$ are also luminescent, and the emission efficiency was quantified for the 3:1 solution stoichiometry.

Syntheses of the Ligands PyboxOMe, PyboxBr, and Pybox and of Their Complexes. Treatment of chelidamic acid with PBr_5 yielded the para-bromo pyridine acid bromide, which undergoes coupling with chloroethylamine hydrochloride in the presence of base to form the amide, as seen in Scheme 1. Cyclization by treating the amide with base in methanol leads to the formation of PyboxOMe. If the cyclization is performed with NaH in THF , PyboxBr forms instead. The targeted ligands are then purified by flash chromatography and can be obtained in overall 36% and 18% yield, respectively, from chelidamic acid as white crystalline solids.

Underivatized Pybox is obtained in a similar way to PyboxBr, but starting from dipicolinic acid, as shown in Scheme 2. Dipicolinic acid is treated with PBr_5 to yield the acid bromide, which then undergoes coupling with chloroethylamine hydrochloride in the presence of base to form the amide. Cyclization in the presence of NaH/THF yields the ligand Pybox in 43% yield from dipico-

linic acid, as a white crystalline solid after purification by flash chromatography.

Treatment of the ligands with lanthanide salts such as the nitrates or triflates in acetonitrile, chloroform, dichloromethane, or methanol yielded luminescent solutions, thus showing evidence of the formation of the complexes in solution and of efficient energy transfer from ligand to lanthanide ion. X-ray quality crystals could be grown for complexes of all the ligands, with the isolated crystals displaying various ligand-to-metal ion stoichiometries, depending on the initial solution composition. The existence of the 1:1, 2:1, and 3:1 stoichiometries for all ligands in solution is seen through absorption and fluorescence titrations, as will be discussed below in the Solution Speciation Section. Since quantitative emission measurements were performed on solutions with a 3:1 stoichiometry, evidence for the formation of this species in solution is presented in the following.

All three ligands react with lanthanide salts in a 3:1 stoichiometry to form a species in which the metal ion is coordinated to three ligands. Such species are seen by NMR and ESI-MS. To facilitate assignments in the NMR spectra, the diamagnetic ions $\text{La}(\text{III})$ or $\text{Lu}(\text{III})$ were utilized instead of the paramagnetic $\text{Eu}(\text{III})$ and $\text{Tb}(\text{III})$, used for the remaining spectroscopic studies. In Figure 1, the ^1H NMR spectra of PyboxOMe and of the diamagnetic $\text{La}(\text{III})$ ion in the presence ligand in various ligand-to-metal ion stoichiometries are shown. The oxazoline proton resonances for the free ligand are found in the region 4.0 to 4.5 ppm. Upon metal coordination these resonances suffer the most dramatic changes,

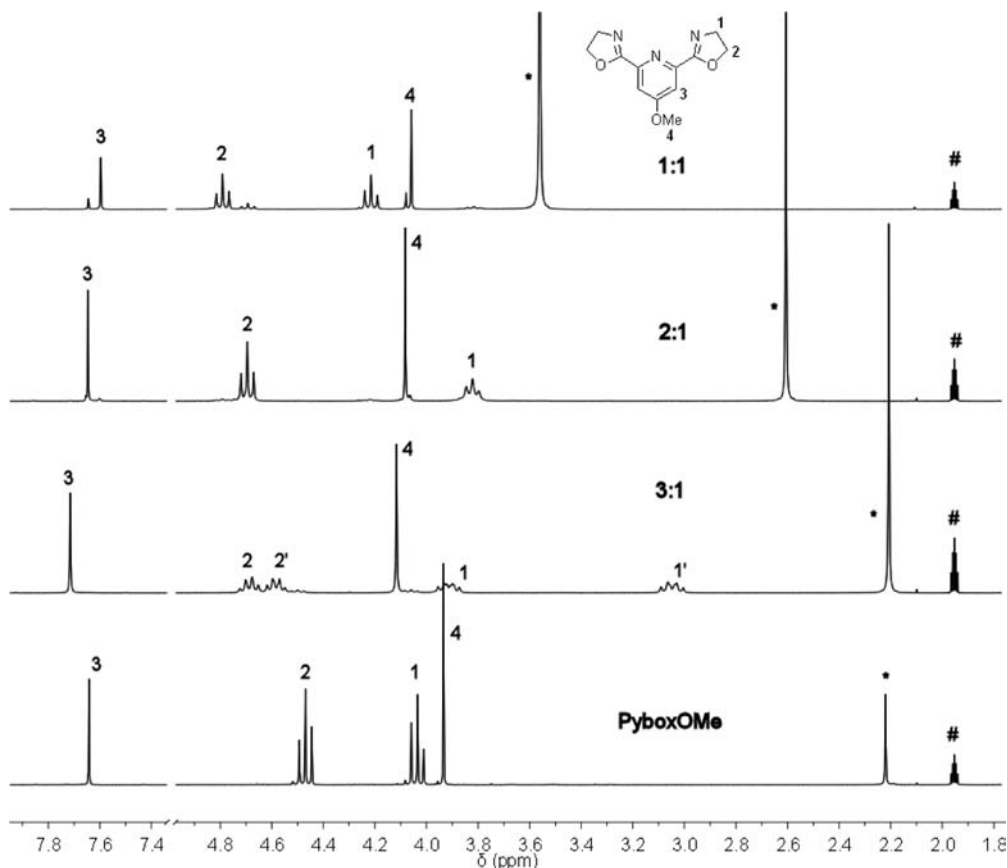


Figure 1. ^1H NMR spectra of PyboxOMe (bottom spectrum) and with La(III) as the triflate salt in different ligand-to-metal stoichiometries in CD_3CN with peak assignments. *Denotes the water and # the CD_3CN resonances.

especially in the case of the 3:1 solution species, for which a large shift is observed; the resonances corresponding to the protons closest to the lanthanum shift upfield and the others downfield. The resonances for the oxazoline protons are the result of a diastereotopic AA'XX' spin system, consistent with the pseudo- D_3 helical symmetry observed in the solid state (see X-ray crystallographic discussion below) being maintained in solution.^{37,38} For comparison, it can be seen that the oxazoline proton pattern simplifies for 2:1 and 1:1 species in solution, indicating different symmetries of the complexes as well as rapid exchange of the ligands on the NMR time scale. The resonances corresponding to aromatic and methyl protons experience only slight shifts upon metal ion coordination for all species. It is further worth noting the presence of a water resonance at ~ 2.2 ppm for both the ligand alone as well as, not shifted, for the 3:1 species, indicating saturation of the coordination sphere of the La(III) by the three PyboxOMe ligands and thus lack of coordination of the water molecules to the metal ion. In the case of the 2:1 and 1:1 species, this peak shifts considerably downfield, indicating that the coordination sphere is not saturated by Pybox-based ligands and thus water molecules are able to coordinate to the metal ion. Similar spectra comparing the free ligands PyboxBr and Pybox with the 3:1 species and thus providing evidence of the sole presence of the 3:1 species in

the solutions utilized for photophysical characterization are displayed in Supporting Information, Figures S1 and S2.

Mass spectral data also show the formation of the 3:1 species, as the molecular ion peaks at 297.82 m/z for the $[\text{Eu}(\text{PyboxOMe})_3]^{3+}$ and at 300.38 m/z for the $[\text{Tb}(\text{PyboxOMe})_3]^{3+}$ complex cations are seen (Figure 2). In the mass spectra of both complexes one additional fragment could be assigned to the $[\text{Ln}(\text{PyboxOMe})_3\text{NO}_3]^{2+}$ species. Similar evidence is found for the ligands PyboxBr and Pybox and is summarized in the Experimental Section.

In the case of the ligand PyboxOMe, the 3:1 stoichiometry was also the one for which X-ray quality crystals were obtained, as discussed in the following.

Structure of Complexes of PyboxOMe with Eu(III), 1, and Tb(III), 2. X-ray quality crystals of compound **1**, a 3:1 structure of PyboxOMe with Eu(III) with the molecular formula $[\text{Eu}(\text{PyboxOMe})_3](\text{NO}_3)_3 \cdot 3\text{CH}_2\text{Cl}_2$, were isolated within a few days of stirring $\text{Eu}(\text{NO}_3)_3$ with the ligand in the appropriate stoichiometry in dichloromethane, followed by filtration and slow solvent evaporation. Crystals of the isostructural Tb(III) complex **2** were isolated in a similar way. The structure of the representative Eu(III) complex is shown in Figure 3a and details of the crystallographic characterization of both complexes can be found in Table 1. The Eu(III) ion has a coordination number of 9 and is surrounded by three PyboxOMe ligands to yield a distorted tricapped trigonal prism, giving the complex cation a pseudo- D_3 symmetry. The coordination polyhedron is shown in Figure 3b. The faces

(37) Piguet, C.; Williams, A. F.; Bernardinelli, G.; Bünzli, J. C. G. *Inorg. Chem.* **1993**, *32*, 4139–4149.

(38) Friebolin, H. *Basic One- and Two-Dimensional NMR Spectroscopy*, 2nd ed.; VCH: Weinheim, 1993.

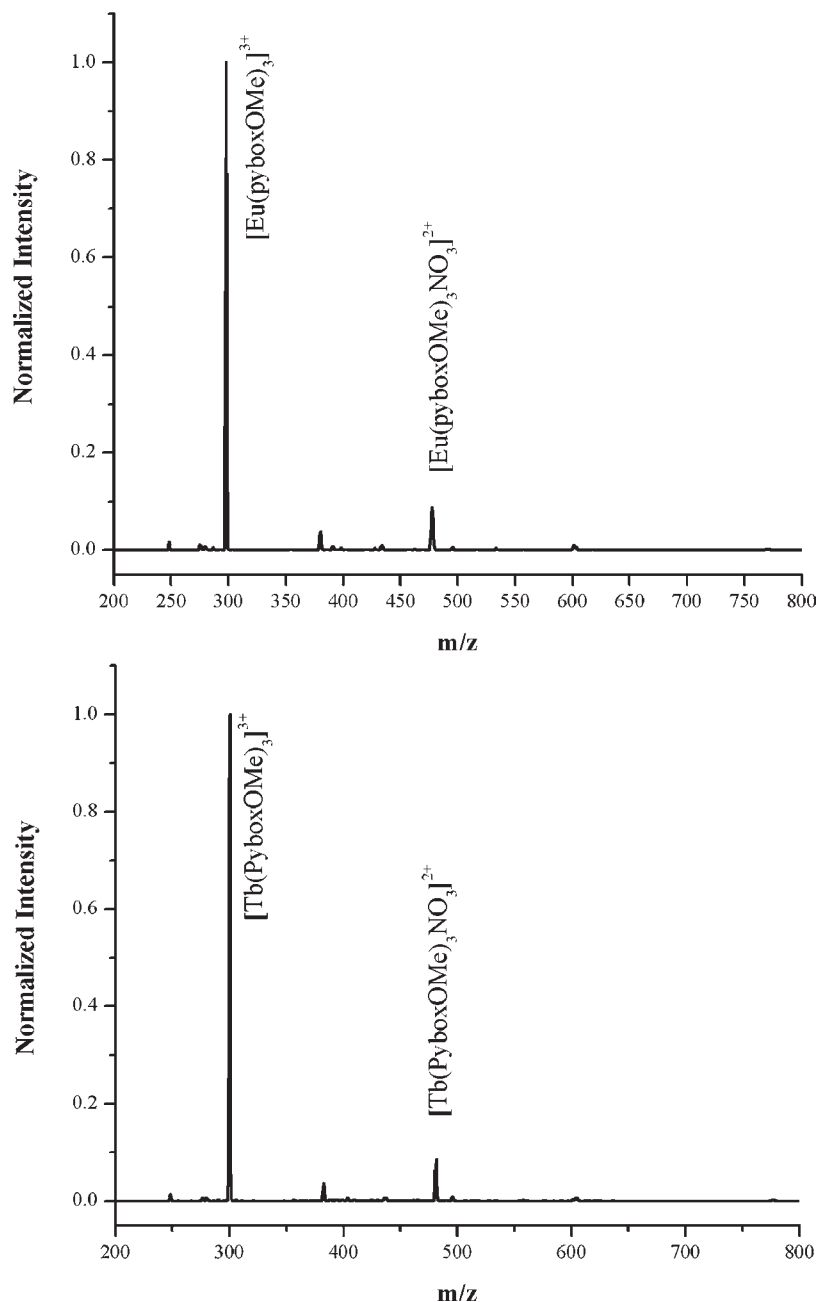


Figure 2. ESI-MS(+) of complexes **1** (top) and **2** (bottom), isolated as solids and then redissolved in acetonitrile.

of the prism are spanned by the nitrogen atoms of the oxazoline rings and are capped by the nitrogen atoms of the pyridine rings. The ligands are flat and almost orthogonal to each other, with torsion angles very close to 0° between pyridine and oxazoline rings. The carbon atoms of the methoxy groups are also in the same plane as the pyridine moiety. Three nitrate ions, shown in Figure 3a, crystallize along with each molecule of complex for charge compensation purposes. Finally, three dichloromethane molecules are also present in the asymmetric unit. One of these molecules is disordered but could be satisfactorily modeled at half occupancy with the other half generated through inversion.

The Eu–N distances are in the range 2.504–2.569 Å, while the isostructural Tb complex shows Tb–N distances in the range 2.484–2.548 Å. These and other selected

bond distances and angles are summarized in the Supporting Information, Tables S1 and S2. The Eu(III)–nitrogen distances are similar to the ones in the range 2.519–2.572 Å seen for the 2:1 complex of Eu(III) with PyboxTh.²⁰

As can be seen in Figure 3, the three ligands assume a helical arrangement around the central metal ion. Despite this arrangement, there is minimal interaction between the individual PyboxOMe ligands, against what is observed for a similar ligand, pyridine-bis(benzimidazolyl).^{37,39} This latter ligand forms triple helical complexes with Ln(III) ions and displays extensive π – π stacking between neighboring ligands, especially because of the presence of

(39) Piguet, C.; Bünzli, J.-C. G.; Bernardinelli, G.; Bochet, C. G.; Froidevaux, P. *J. Chem. Soc., Dalton Trans.* **1995**, 83–97.

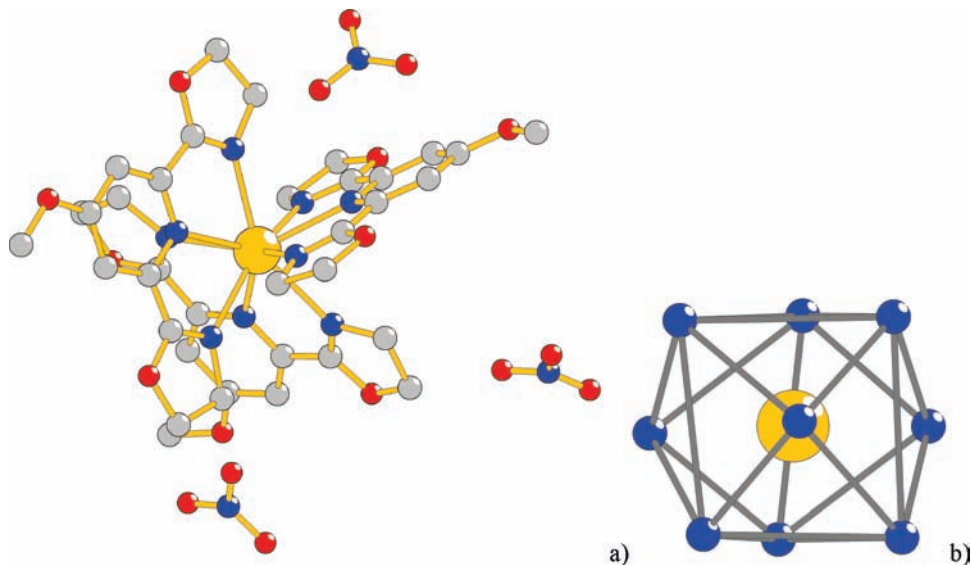


Figure 3. (a) Ball-and-stick diagram of $[\text{Eu}(\text{PyboxOMe})_3](\text{NO}_3)_3 \cdot 3\text{CH}_2\text{Cl}_2$, **1**. Hydrogen atoms and methylene chloride molecules of crystallization were omitted for clarity. (b) Distorted tricapped trigonal prism coordination environment around Eu(III) in the complex.

the benzene moieties on the imidazolyl rings, which are absent in these Pybox derivatives. Further, despite the relatively close proximity of the ligands, the very weak interactions observed between them fall outside of the normally accepted range for weak hydrogen bonding or $\text{C}-\text{H} \cdots \pi$ -interactions (Supporting Information, Figure S3).⁴⁰ Because of the helical ligand arrangement, the crystals contain a racemic mixture of both the Λ and Δ isomers of the complex cation (Supporting Information, Figure S4). A pair of symmetry related dichloromethane molecules is located between each pair of enantiomers and bridge these through $\text{C}-\text{H} \cdots \text{Cl}$ interactions (Supporting Information, Table S3 and Figure S4), with D–A distances of 3.6447 and 3.6855 Å for Eu(III) and 3.6424 and 3.6747 Å for Tb(III). The two enantiomers are further bridged by a nitrate ion, which weakly hydrogen-bonds with two oxazoline rings on one enantiomer and one methyl moiety on the other. The D–A distances are in the range 3.2450–3.4008 Å for Eu(III) and 3.2446–3.3778 Å for Tb(III). Weak hydrogen bonding interactions are also present between this nitrate anion and the disordered dichloromethane molecule, as well as between other nitrates and oxazoline rings and nitrates and dichloromethane molecules. Dissolution of crystals obtained for crystallography yields ESI-MS spectra equivalent to the ones in Figure 2 (Supporting Information, Figure S5).

Structures of Complexes of PyboxBr with Eu(III), 3, and Tb(III), 4. Complexes of PyboxBr with $\text{Eu}(\text{NO}_3)_3$ were isolated within a few days after refluxing the ligand with the metal salt in the desired stoichiometry in methanol, removal of the solvent and dissolution of the residue in a minimum amount of acetonitrile and slow evaporation of the solvent. Two structures were obtained with this ligand. The asymmetric unit of the first one, $[\text{EuPyboxBr}(\text{NO}_3)_3(\text{H}_2\text{O})]$, **3**, is shown in Figure 4a. Details of the crystallographic characterization are summarized

in Table 1 and selected bond distances and angles can be found in Table S4 for complex **3** and Table S5 for **4**, the complex with the molecular formula $[\text{Tb}(\text{PyboxBr})_2(\eta^2\text{-NO}_3)(\eta^1\text{-NO}_3)_2][\text{Tb}(\text{NO}_3)_5] \cdot 5\text{H}_2\text{O}$, in the Supporting Information. In complex **3**, only one ligand is coordinated to the metal ion. One water molecule and three bidentate nitrate anions complete the coordination sphere for a coordination number of 10. The Eu–N distances are in the range 2.557–2.599 Å and the Eu–O distances in the range 2.400–2.565 Å. The PyboxBr ligand is almost flat, as seen in the previous structures, with torsion angles of 0.23 and 5.62°. The geometry around the Eu(III) ion is a highly distorted bicapped square antiprism, shown in Figure 4b. The capping atoms correspond to the pyridine nitrogen and the coordinated water molecule, leaving thus the oxazoline nitrogen and nitrate oxygen atoms to form the top face of the prism and the remaining nitrate oxygen atoms the bottom face.

The packing diagram for **3** is shown in Figure 5. Hydrogen-bonding interactions between the coordinated water of one molecule and the coordinated nitrate anions of adjacent molecules dominate the three-dimensional structure. The hydrogen bonding distances are 2.754–2.865 Å and the O–O–O angle, at 99.56°, is smaller than the expected tetrahedral angle.

While π - π stacking interactions are virtually absent from this structure, $\text{Br} \cdots \pi$ short contacts of 3.632 Å are present between ligands on neighboring molecules, as shown in Supporting Information, Figure S6. The packing structure of this complex is further supported by weak hydrogen bonding interactions in the range 3.2803–3.5734 Å between C–H moieties on the pyridine and oxazoline rings and oxygen atoms of the coordinated nitrate anions (Supporting Information, Figure S7).

Of all the compounds discussed in this manuscript the one with the most unexpected structure is **4**. While attempting to isolate a 2:1 species in the solid state this compound, $[\text{Tb}(\text{PyboxBr})_2(\eta^2\text{-NO}_3)(\eta^1\text{-NO}_3)_2][\text{Tb}(\text{NO}_3)_5] \cdot 5\text{H}_2\text{O}$, **4**, crystallized as a racemic twin in the $P2_1$ monoclinic space group. Its structure is shown in Figure 6.

(40) Desiraju, G.; Steiner, T., *The Weak Hydrogen Bond In Structural Chemistry and Biology*; Oxford University Press: New York, 1999; Vol. 9, p 528.

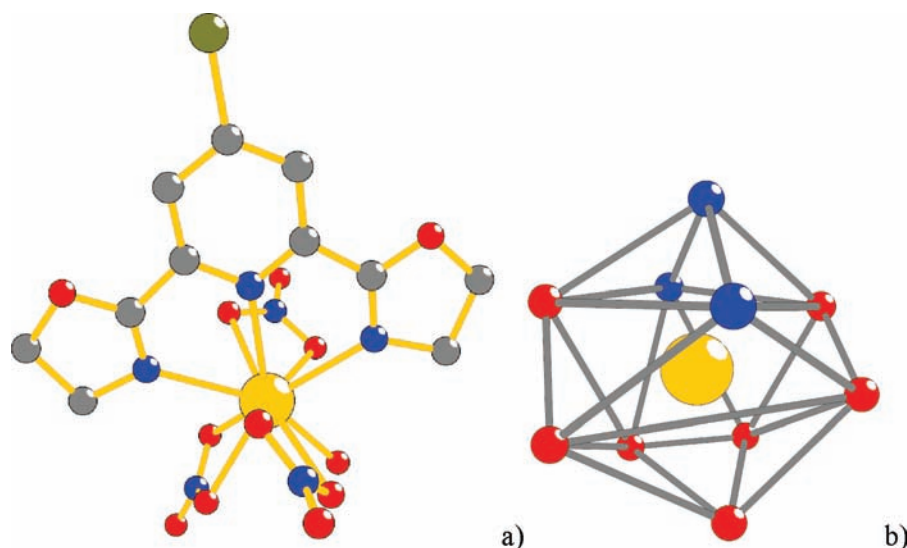


Figure 4. Ball-and-stick representations of (a) **3**, the 1:1 complex of PyboxBr with $\text{Eu}(\text{NO}_3)_3$ and (b) the highly distorted bicapped square antiprism coordination polyhedron around $\text{Eu}(\text{III})$. Hydrogen atoms have been omitted for clarity.

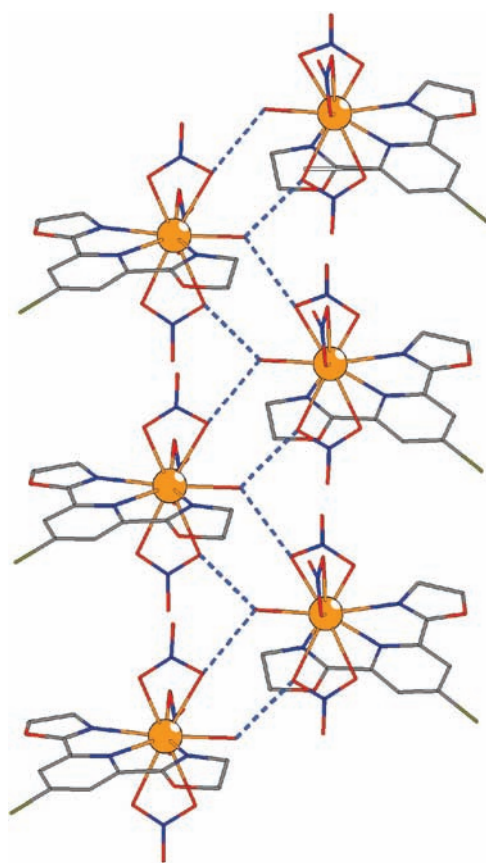


Figure 5. Wire representation of the packing structure of **3**, showing the hydrogen-bonding network between the water molecule coordinated to the $\text{Eu}(\text{III})$ of one molecule interacting with the nitrate anion oxygen atoms of two adjacent molecules. Hydrogen atoms have been omitted for clarity. Hydrogen bonding distances (Å) and angles (deg) are: $\text{O12}(\text{water}) \cdots \text{O7}(\text{nitrate})$ 2.754, $\text{O12}(\text{water}) \cdots \text{O10}(\text{nitrate})$ 2.865, $\text{O7}-\text{O12}-\text{O10}$ 99.56.

In the asymmetric unit two $\text{Tb}(\text{III})$ ions, each surrounded by two PyboxBr, are present. These two metal ions are further coordinated to one bidentate and one monodentate nitrate anion. The coordination number is

in both cases 9, and the coordination polyhedra, shown in Supporting Information, Figure S8, can be approximated to distorted tricapped trigonal prisms. Since these two $\text{Tb}(\text{III})$ -containing species display a positive charge, charge balancing is provided by a third $\text{Tb}(\text{III})$ ion surrounded by five bidentate nitrate anions, with a coordination number of 10. The coordination polyhedron around this metal ion is best described by a bicapped square antiprismatic geometry and is shown in Supporting Information, Figure S8c. The $\text{Tb}-\text{N}$ distances for the first two $\text{Tb}(\text{III})$ ions are in the range 2.506–2.880 Å, and the $\text{Tb}-\text{O}$ distances for all three metal ions are in the range 2.332–2.555 Å. Four water molecules of crystallization are also present in a disordered fashion in a small cavity spanned by the three complex ions (Supporting Information, Figure S9). These four molecules participate in an extensive hydrogen bond and weak hydrogen bond network which supports the packing structure of the complex with $\text{D}-\text{H} \cdots \text{A}$ distances in the range 2.0112–2.9995 Å ($\text{H} \cdots \text{A}$) for $\text{D} = \text{C}$ and in the range 2.0743–3.9150 Å ($\text{D} \cdots \text{A}$) for $\text{D} = \text{O}$ (Supporting Information, Table S6).

Structures of Complexes of Pybox with $\text{Tb}(\text{III})$ in the 3:1 Stoichiometry, **5, and 2:1 Stoichiometry, **6**.** Complexes **5** and **6** are examples of coordination compounds isolated with the underivatized Pybox ligand. Complex **5** has the molecular formula $[\text{Tb}(\text{Pybox})_3](\text{CF}_3\text{SO}_3)_3 \cdot 3\text{CH}_3\text{CN}$ and displays a 3:1 ligand stoichiometry. Its structure is shown in Figure 7, and details of the crystallographic characterization are summarized in Table 1, while selected bond distances and angles can be found in Supporting Information, Table S7. It crystallizes in the triclinic space group $P\bar{1}$ with two metal ion containing molecules in the unit cell. Because of the 3:1 stoichiometry, in analogy to compound **1**, the ligands are arranged in a helical fashion around the metal ion leading to the presence of both Λ and Δ isomers in the unit cell with pseudo- D_3 symmetry.

The two enantiomers are separated by triflate counteranions as well as the acetonitrile solvent molecules (not shown). The $\text{Tb}(\text{III})$ ions are nine-coordinate in a tricapped

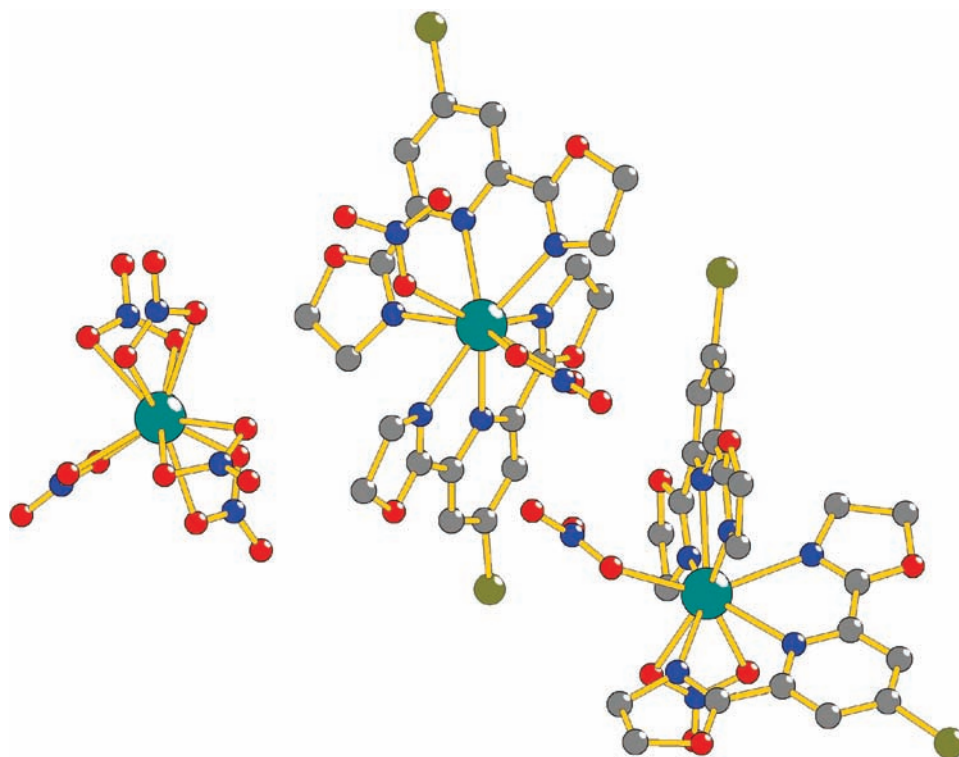


Figure 6. Ball-and-stick representation of $[\text{Tb}(\text{PyboxBr})_2(\eta^2\text{-NO}_3)(\eta^1\text{-NO}_3)_2][\text{Tb}(\text{NO}_3)_5] \cdot 5\text{H}_2\text{O}$, **4**. Hydrogen atoms and water molecules of crystallization were omitted for clarity.

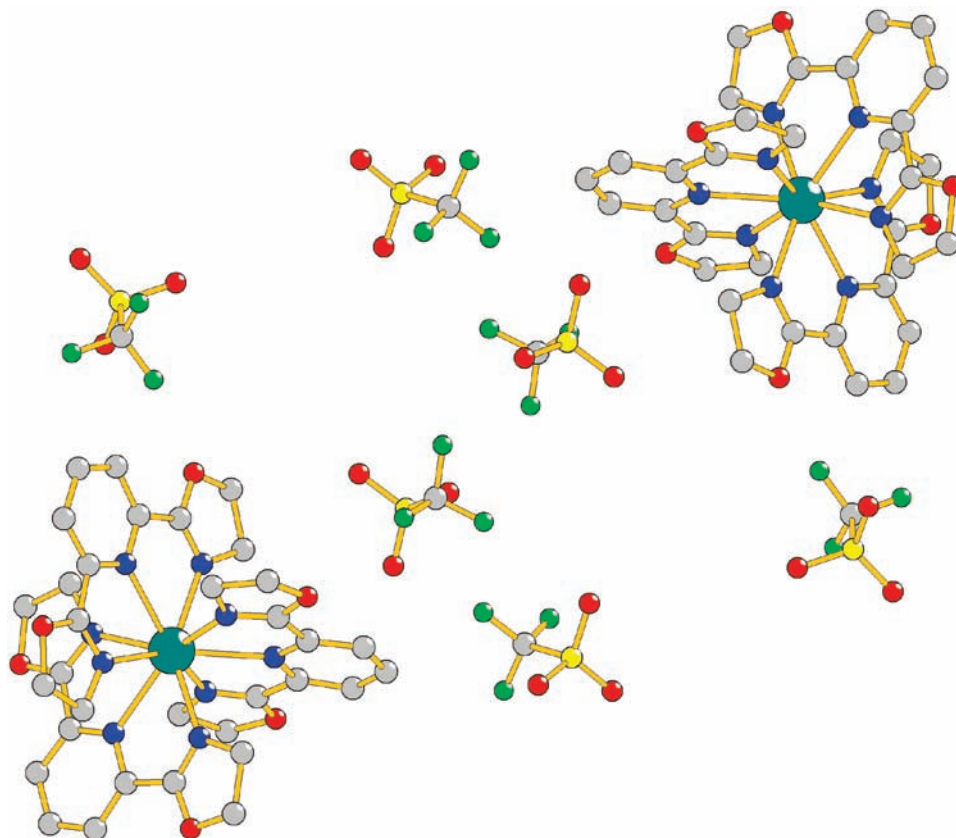


Figure 7. Ball-and-stick diagram of $[\text{Tb}(\text{Pybox})_3](\text{CF}_3\text{SO}_3)_3 \cdot 3\text{CH}_3\text{CN}$, **5**. Hydrogen atoms and acetonitrile molecules of crystallization were omitted for clarity. The Λ (top right) and Δ (bottom left) isomers present in the structure can be seen.

trigonal prismatic coordination environment (Supporting Information, Figure S10), in which the faces of the prism are

spanned by the oxazoline nitrogen atoms and the capping nitrogen atoms belong to the pyridine rings, with Tb–N

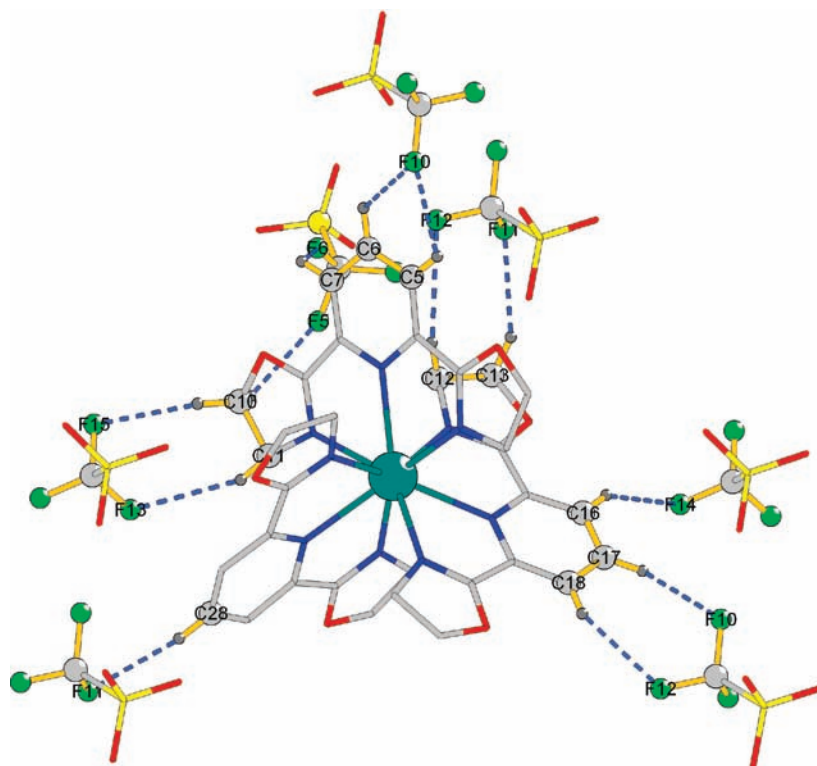


Figure 8. Diagram displaying the hydrogen-bonding interactions between the triflate molecules and the complex molecule of **5**. Selected bond distances C–H····F and C····F [Å] and angles C–H····F [deg] are: C10····F5 2.588, 3.303, 129.1, C10····F15, 2.455, 3.439, 172.1, C7····F5 2.769, 3.312, 117.7, C11····F13 2.735, 3.451, 129.5, C16····F14 2.642, 3.497, 149.9, C5····F10 2.523, 3.163, 124.7, C6····2.792, 3.297, 114.2, C12····F12 2.859, 3.797, 153.3, C13····F11 2.521, 3.419, 150.7, C17····F10 2.550, 3.318, 138.1, C18····F12 2.527, 3.324, 141.5, C28····F11 2.549, 3.482, 167.5.

distances in the range 2.4953–2.5497 Å, which are comparable to the bond distances in complex **2**, which also has 3:1 stoichiometry. The triflate molecules are involved in extensive hydrogen-bonding, as previously seen for the molecule isolated with PyboxTh.²⁰ Each complex cation is surrounded by 7 triflate anions, as seen in Figure 8, and C–H····F interactions show D····A distances in the range 3.1629–3.7697 Å (D–H····A 2.5207–2.8589 Å).

These interactions support the three-dimensional packing structure of the complex, as can be seen in Supporting Information, Figures S11–S13. Weak C–H····O hydrogen bonding interactions between oxazoline ring and triflate oxygen atoms and C–H groups on the acetonitrile molecules of crystallization and adjacent pyridine and oxazoline rings are also present and contribute to the packing structure, as shown in Supporting Information, Figure S13. The C–H····O distances are in the range 2.4042–2.9615 Å and are summarized in Supporting Information, Table S8.

Complex **6** crystallizes in the triclinic $P\bar{1}$ space group. This complex displays two ligands coordinated to the Tb(III) ion, along with one nitrate anion and one water molecule. The coordination number is thus 9, and the coordination polyhedron around the metal ion is a distorted monocapped square antiprism. A drawing of the complex, without the unbound nitrate counter-anions and solvent molecules, is displayed in Figure 9a, and the coordination polyhedron is drawn in Figure 9b. The base of the antiprism is spanned by the nitrogen atoms of pyridine and oxazoline rings, while the top face comprises the two nitrogen atoms of the two remaining oxazoline

rings and oxygen atoms of the one nitrate oxygen atom and the water molecule. The capping atom is the second oxygen atom of the bidentate nitrate counteranion. The Tb–N distances are in the range 2.483–2.877 Å, the Tb–O bonds lengths are in the range 2.343–2.464 Å, and both are summarized in Supporting Information, Table S9.

An extensive hydrogen bonding network is present in this molecule between nitrate counterions and methanol molecules of solvation and the complex molecules (Supporting Information, Figure S14). The D–H····A distances are in the range 2.3378–2.9774 Å and are summarized in Supporting Information, Table S10.

Solution Speciation and Structure of the 3:1 Species.

As mentioned above, the existence in solution of the 3:1 ligand-to-metal ion species for all three ligands is supported by NMR spectroscopy as well as ESI-MS data. This stoichiometry is further encountered in the solid state, as seen for structures **1**, **2**, and **5**. Structures **3**, **4**, and **6**, on the other hand, display 1:1 and 2:1 stoichiometries. These different ligand-to-metal ion ratios are also present in solution, under the appropriate experimental conditions. We have therefore studied the speciation of the metal ion complexes in solution by fluorescence and absorption titrations. The measurements were performed in acetonitrile solution at constant ionic strengths with either nitrate or triflate salts of the lanthanide ions. The stability constants $\log \beta$ obtained from these measurements are summarized in Table 2. Sample titration spectra for all ligands and metal ions are shown in Figure 10 as well as Supporting Information, Figures S15–S20. In Figure 10 a typical absorption titration, exemplified for Pybox with Tb(III), is shown.

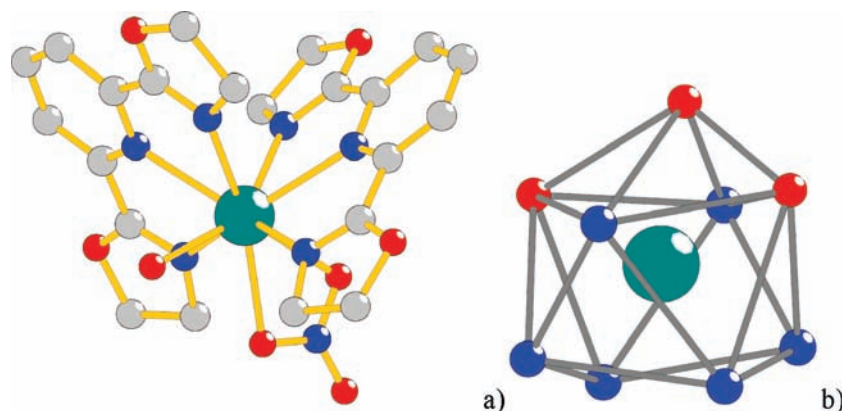


Figure 9. Ball-and-stick representations of (a) **6**, the 2:1 complex of Pybox with $\text{Tb}(\text{NO}_3)_3$ and (b) the distorted monocapped square antiprism coordination polyhedron around $\text{Tb}(\text{III})$. Hydrogen atoms, nitrate counterions, and methanol molecules of crystallization have been omitted for clarity.

Table 2. Stability Constants for the $[\text{Ln}(\text{PyboxR})_n]^{3+}$ ($\text{R} = \text{Br}, \text{H}, \text{OMe}, \text{Th}^a$) Complex Cations ($\text{Ln} = \text{Eu}, \text{Tb}, n = 1, 2, 3$) Determined in Acetonitrile Solution at Constant Ionic Strength ($I = 0.1 \text{ M Et}_4\text{NCl}$) by Emission (FL) and Absorption (UV) Spectroscopy

R	Ln		$\log \beta_{11}$	$\log \beta_{21}$	$\log \beta_{31}$	average $\log \beta_{11}^d$	average $\log \beta_{21}^d$	average $\log \beta_{31}^d$
OMe^b	Eu	UV	4.89 ± 0.09	8.08 ± 0.20	11.86 ± 0.83	5.4 ± 0.1	8.8 ± 0.4	12.8 ± 1.0
		FL	5.80 ± 0.10	9.46 ± 0.31	13.80 ± 0.53			
	Tb	UV	4.45 ± 0.20	8.71 ± 0.15	11.57 ± 0.18	4.5 ± 0.5	8.4 ± 0.5	11.7 ± 0.6
		FL	4.48 ± 0.42	8.00 ± 0.44	11.79 ± 0.57			
H^c	Eu	UV	3.61 ± 0.15	9.12 ± 0.19	11.99 ± 0.11	3.6 ± 0.2	9.1 ± 0.2	12.0 ± 0.2
		FL	3.64 ± 0.08	9.15 ± 0.10	11.97 ± 0.12			
	Tb	UV	3.68 ± 0.06	9.34 ± 0.23	12.27 ± 0.31	3.7 ± 0.2	9.3 ± 0.4	12.2 ± 0.3
		FL	3.70 ± 0.22	9.34 ± 0.26	12.03 ± 0.10			
Br^c	Eu	UV	7.04 ± 0.06	12.56 ± 0.17	16.74 ± 0.22	7.1 ± 0.2	12.2 ± 0.2	15.5 ± 0.3
		FL	7.14 ± 0.20	11.73 ± 0.17	14.31 ± 0.16			
	Tb	UV	6.07 ± 0.05	11.16 ± 0.26	15.39 ± 0.56	6.2 ± 0.2	11.0 ± 0.4	15.4 ± 0.6
		FL	6.32 ± 0.21	10.80 ± 0.23	15.47 ± 0.22			
$\text{Th}^{a,c}$	Eu				5.2 ± 0.2	10.4 ± 0.2	14.9 ± 0.2	
	Tb				4.9 ± 0.2	9.1 ± 0.1	12.7 ± 0.2	

^a Shown here for comparison, from reference 20. ^b Ln as the triflate salt. ^c Ln as the nitrate salt. ^d Average of emission and absorption measurements with propagated uncertainty.

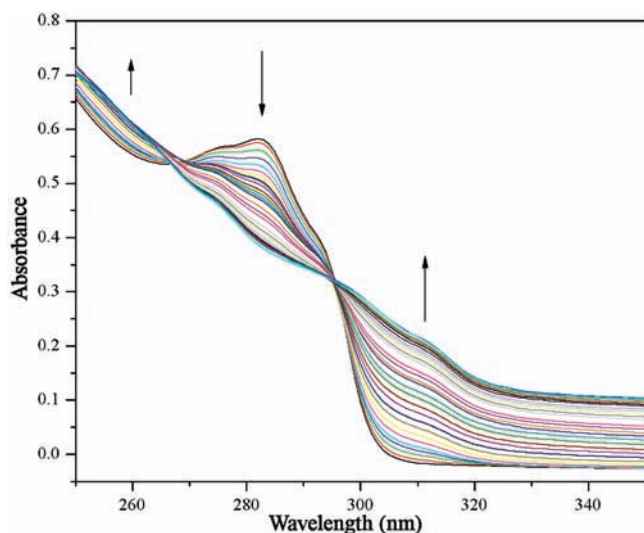


Figure 10. Absorption titration experiment of Pybox in acetonitrile with $\text{Tb}(\text{NO}_3)_3$ performed at constant ionic strength $I = 0.1 \text{ M Et}_4\text{NCl}$; $[\text{Ln}(\text{Pybox})_3]^{3+} = 1 \times 10^{-4} \text{ M}$.

The initial trace corresponds to the ligand absorption and upon successive additions of lanthanide ion salt solution, the peak at 280 nm decreases, while features below 260 and above 300 nm increase in intensity. As discussed below, and based on

the NMR data presented above, four different species will be present during the titration experiment. However, only two isosbestic points are seen, which is due to the highly correlated nature of the absorption behavior of all four species.^{20,21,41}

The stability constants have values of $\log \beta_{11}$ in the range 3.6–7.1, $\log \beta_{21}$ in the range 8.4–12.2, and $\log \beta_{31}$ in the range 11.7–15.5. They are comparable to the previously described PyboxTh species, shown also in Table 2. Albeit of the same magnitude, the stability constants are smaller than the values reported for a chiral derivative of bis(benzimidazole)pyridine.⁴² This ligand displays stability constants of 8.2, 14.1, and 18.1 for the formation of the 1:1, 2:1 and 3:1 species, respectively, with $\text{Eu}(\text{III})$. The higher stability might be a consequence of the stabilizing effect of the intramolecular π – π interactions in the bis(benzimidazole)pyridine systems, which are absent in the case of the Pybox derivatives discussed here, as well as a modulation of the cavity size by the presence of the functional groups on the imidazole nitrogen atom. Surprisingly, the stability constants for the Pybox-based complexes are also slightly smaller than stability constants reported for terpyridine complexes, which have

(41) Comby, S.; Imbert, D.; Chauvin, A.-S.; Bünzli, J.-C. G.; Charbonnière, L. J.; Ziessel, R. F. *Inorg. Chem.* **2004**, *43*, 7369–7379.

(42) Müller, G.; Bünzli, J.-C. G.; Schenk, K. J.; Piguet, C.; Hopfgartner, G. *Inorg. Chem.* **2001**, *40*, 2642–2651.

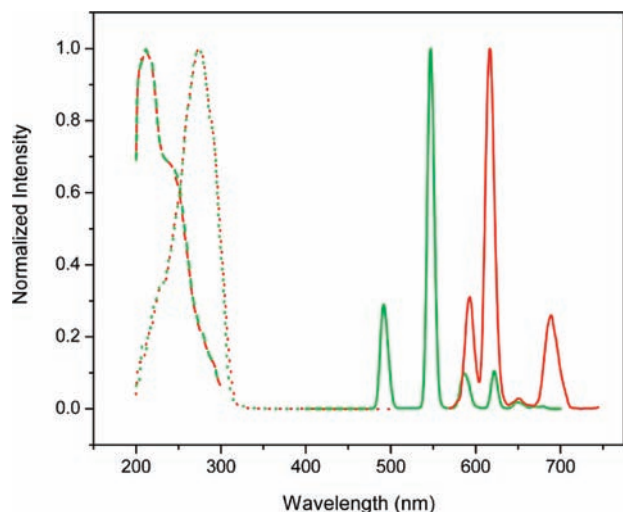


Figure 11. Absorption (dashed), excitation (dotted), and emission (solid) spectra of $[\text{Eu}(\text{PyboxOMe})_3]^{3+}$ (red) and $[\text{Tb}(\text{PyboxOMe})_3]^{3+}$ (green) measured with the nitrate salts in acetonitrile solution and $[\text{Ln}(\text{III})] \approx 1 \times 10^{-4}$ M.

been noted to be unstable in the 3:1 stoichiometry in solution.^{35,43} Overall, and within experimental error, the stability constants are very similar for all compounds described here. It is well-known that despite the similar sizes of the lanthanide ions, a fine-tuning of the complexation can still be achieved and that not all chelating ligands will accommodate different lanthanide ions equally well. In the case of the data presented here, no such trend is visible. This is most likely due to the highly correlated nature of the absorbing and emitting species; the errors associated with the determination of the stability constants are high and prevent a more precise calculation of the $\log \beta$ values. Nonetheless, the data indicate that PyboxBr forms the more stable complex cations in solution. This is surprising as this ligand, because of the electron-withdrawing nature of the bromide substituent, should be the least basic. Further studies with other substituents at the para position of the pyridine ring are currently underway to shed light on this apparent discrepancy.

Photophysical Characterization of the 3:1 Species on Solution. All complexes are luminescent in the solid state and in solution, in solvents such as acetonitrile, chloroform, dichloromethane, and methanol. Representative spectra of the absorption, emission, and excitation of PyboxOME complexes of both the Eu(III) and the Tb(III) analogues are shown in Figure 11, while the analogous data for the Pybox and PyboxBr ligands are shown in Supporting Information, Figures S21 and S22, respectively. All three ligands absorb strongly in the UV with maxima at $\lambda = 236, 231,$ and 227 nm for Pybox, PyboxBr, and PyboxOME, respectively. Upon complexation to a lanthanide ion, the absorption maxima are 240, 245, and 240 nm. The shapes of the absorption and excitation spectra (excitation maxima at 272, 249, and 273 nm) are virtually identical for the complexes of both metals, with the excitation spectra displaying small bathochromic shifts with respect to the absorption. The similarity of absorption and excitation spectra is consistent with

sensitization of the lanthanide emission through absorption of light by the ligand and subsequent energy transfer to the lanthanide ion. The emission spectra show the characteristic peaks for each metal ion, ${}^5\text{D}_0 \rightarrow {}^7\text{F}_J$ ($J = 1, 2, 3, 4$) for Eu(III) and ${}^5\text{D}_4 \rightarrow {}^7\text{F}_J$ ($J = 6, 5, 4, 3, 2$) for Tb(III). In the case of Eu(III) complexes, the relative intensities of the magnetic dipole forbidden ${}^5\text{D}_0 \rightarrow {}^7\text{F}_2$ and the magnetic dipole allowed ${}^5\text{D}_0 \rightarrow {}^7\text{F}_1$ transitions relate directly to the symmetry around the central metal ion.^{44,45} In the three species described here, the ratio does not change appreciably, indicating that the coordination sphere has a very similar arrangement in all three 3:1 species.

The efficiency of the emission was determined for the 3:1 species in acetonitrile solution with both nitrate and triflate salts of the lanthanide ions. The data are summarized in Table 3, along with the singlet and triplet state energies of the ligands, as well as excited state lifetimes in acetonitrile, methanol and deuterated methanol.

The singlet state energies are above $30,000 \text{ cm}^{-1}$ for all three ligands, with PyboxOME displaying the highest and Pybox the lowest level. The triplet state energies are $\sim 26,000 \text{ cm}^{-1}$ for PyboxOME, $\sim 25,000 \text{ cm}^{-1}$ for Pybox, and $\sim 23,300 \text{ cm}^{-1}$ for PyboxBr, following a general trend of a lower energy with increasing electron-withdrawing ability of the functional group at the para position of the pyridine ring. These triplet levels are thus in appropriate position⁴⁶ to transfer energy to the excited states of Eu(III), situated at $\sim 17,300 \text{ cm}^{-1}$, and Tb(III), at $\sim 20,500 \text{ cm}^{-1}$. PyboxBr, which has the lowest triplet state energy, also displays the highest quantum efficiency for Eu(III) emission at 35.8%. The other ligands, which display a larger triplet-f excited state gap, have similar emission efficiencies of 23.5 and 25.6% for PyboxOME and Pybox, respectively. These findings are consistent with observations reported on *p*-chloro-, *p*-hydroxy-, and underivatized pyridine-2,6-dicarboxylic acid. While neither triplet energy levels nor emission quantum yields were determined for the complexes, a decrease in Eu(III) emission intensity was seen with increasing electron-withdrawing ability of the para-substituent substituent.⁴⁷ In the case of Tb(III) emission, the efficiencies reported here are around 21–23% and are within experimental error the same for all three systems. This is in contrast with the reported emission efficiencies of complexes of Tb(III) sensitized by *p*-bromo-, *p*-hydroxy-, and underivatized pyridine-2,6-dicarboxylic acid. For those ligands, the efficiency is highest for the hydroxy-substituted ligand, with the *p*-bromo-substituted ligand having the lowest efficiency.⁴⁸ Gassner et al., who compared underivatized pyridine-2,6-dicarboxylic acid with *p*-methoxy-pyridine-2,6-dicarboxylic acid, noted a decrease in the emission efficiency for both Eu(III) and Tb(III), in the presence of the electron-donating OMe moiety.⁴⁴ The previously described ligand PyboxTh, with a more favorable triplet state energy of $\sim 21,000 \text{ cm}^{-1}$,

(44) Gassner, A.-L.; Duhot, C.; Bünzli, J.-C. G.; Chauvin, A.-S. *Inorg. Chem.* **2008**, *47*, 7802–7812.

(45) Klink, S. I.; Hebbink, G. A.; Grave, L.; Oude Alink, P. G. B.; van Veggel, F. C. J. M.; Werts, M. H. V. *J. Phys. Chem. A* **2002**, *106*, 3681–3689.

(46) Latva, M.; Takalo, H.; Mikkala, V.-M.; Matachescu, C.; Rodriguez-Ubis, J. C.; Kankare, J. *J. Lumin.* **1997**, *75*, 146–169.

(47) George, M. R.; Golden, C. A.; Gossel, M. C.; Curry, R. J. *Inorg. Chem.* **2006**, *45*, 1739–1744.

(48) Lamture, J. B.; Zhou, Z. H.; Kumar, A. S.; Wensel, T. G. *Inorg. Chem.* **1995**, *34*, 864–869.

(43) Mürmer, H.-R.; Chassat, E.; Thummel, R. P.; Bünzli, J.-C. G. *Dalton Trans.* **2000**, 2809–2816.

Table 3. Quantum Yields of Luminescence Φ , Excited State Lifetimes τ of the 3:1 Species, Number of Coordinated Solvent Molecules q and Ligand Singlet and Triplet States, Measured with the Metal Ion Nitrates at 1×10^{-4} M Concentration^a

	Ln(III)	PyboxOMe	Pybox	PyboxBr
$E(^1S)$ (cm ⁻¹)		33,220 ± 300	31,790 ± 90	33,110 ± 230
$E(^3T)$ (cm ⁻¹)	Gd	25,950 ± 120	24,940 ± 150	23,260 ± 70
Φ (%) ^b	Eu	23.5 ± 1.6 (24.4 ± 2.2)	25.6 ± 1.1 (24.2 ± 3.0)	35.8 ± 1.6 (32.2 ± 4.5)
	Tb	21.4 ± 3.6 (23.9 ± 2.9)	23.2 ± 2.1 (26.1 ± 1.8)	23.3 ± 1.3 (21.9 ± 2.6)
τ (ms) ^{b,c}	Eu	1.54 ± 0.04 (1.73 ± 0.36)	1.49 ± 0.04 (1.74 ± 0.29)	1.46 ± 0.03 (1.59 ± 0.17)
	Tb	1.88 ± 0.04 (1.29 ± 0.10)	0.44 ± 0.01 (1.05 ± 0.10)	0.79 ± 0.05/0.07 ± 0.01 (1.14 ± 0.40/0.35 ± 0.04)
τ (ms) ^d	Eu	1.95 ± 0.23	1.81 ± 0.22	1.70 ± 0.19
	Tb	1.60 ± 0.04	1.42 ± 0.22	1.34 ± 0.15/0.67 ± 0.06
τ (ms) ^e	Eu	2.46 ± 0.09	2.04 ± 0.22	2.33 ± 0.11
	Tb	1.63 ± 0.04	1.55 ± 0.23	1.43 ± 0.16/0.44 ± 0.04
q	Eu	0.24 ± 0.12	0.14 ± 0.11	0.34 ± 0.11
	Tb	0.10 ± 0.04	0.50 ± 0.34	0.37 ± 0.05

^a Reported as the 0–0 transition from ligand fluorescence and phosphorescence measurements as Gd(III) complexes at 77 K.³⁴ ^b Triflate salts in parentheses. ^c Measured in acetonitrile. ^d Measured in methanol. ^e Measured in CD₃OD.

compared to the Pybox derivatives described here, shows a more efficient energy transfer process, with quantum yields of 76.2 and 58.6% for Eu(III) and Tb(III), respectively. Terpyridine, a ligand which is structurally related to pyridine-bis(oxazoline), has been reported to have singlet and triplet states located at 26,700 and 21,200 cm⁻¹, respectively.⁴³ Its Eu(III) and Tb(III) 3:1 complexes, despite the appropriately located singlet and triplet excited states, only display quantum yields of 1.3⁴⁹ and 4.7%,⁵⁰ respectively.

The excited state lifetimes for the systems discussed here are unremarkable and similar to values reported in the literature for other lanthanide ion complexes in the same solvents.^{39,43,47,51} They are also largely independent of the solvent utilized, providing further evidence of the stability of the 3:1 species in solution and lack of solvent coordination to the metal ion, seen in the NMR spectra. This was further supported by determining the number of coordinated methanol molecules using Horrocks' equation⁵² and lifetime measurements in methanol and deuterated methanol. Values close to zero were obtained for all complexes showing, within experimental error, that methanol does not coordinate to the metal ion in solution when the ion is protected by the coordinated ligand molecules. It is interesting to note that the PyboxBr ligand leads to double exponential decay of the Tb(III) emission. A similar behavior had been previously observed for the PyboxTh ligand, which also led to a double exponential decay of luminescence for Tb(III). This is attributed to an incomplete energy transfer from the ligand to the excited state of the lanthanide ion and concurrent ligand emission, which has vibronic components in the 400–600 nm region (see Supporting Information, Figure S23). To calculate the number of methanol molecules coordination to the metal ion for this ligand system, only the long lifetime was utilized, as it is the one attributed to the metal containing species.

(49) Petoud, S.; Bünzli, J.-C. G.; Schenk, K. J.; Piguet, C. *Inorg. Chem.* **1997**, *36*, 1345–1353.

(50) Renaud, F.; Piguet, C.; Bernardinelli, G.; Bünzli, J.-C. G.; Hopfgartner, G. *Chem.—Eur. J.* **1997**, *3*, 1646–1659.

(51) Müller, G.; Schmidt, B.; Jiricek, J.; Hopfgartner, G.; Riehl, J. P.; Bünzli, J.-C. G.; Piguet, C. *Dalton Trans.* **2001**, 2655–2662.

(52) Horrocks, W. D., Jr.; Sudnick, D. R. *J. Am. Chem. Soc.* **1979**, *101*, 334–340.

Conclusions

Three chelating ligands based on pyridine-bis(oxazoline), two of which were previously unknown, with different functional groups in the para position of the pyridine ring have been synthesized and characterized. These ligands coordinate readily to lanthanide ions, and do sensitize the luminescence of Eu(III) and Tb(III). In the solid state several different metal complexes with these ligands have been isolated, with examples spanning the whole range of possible ligand-to-metal ion stoichiometries. In solution, evidence was gathered for the selective formation of species with 1:1, 2:1 and 3:1 stoichiometries. All systems, solid and solutions, present the characteristic luminescence of the lanthanide ions, showing an efficient ligand-to-metal ion energy transfer process. Since the 3:1 stoichiometry effectively saturates the coordination sphere of the metal ion, quantitative emission efficiency was measured for solutions with this stoichiometry. Quantum yields of luminescence in the range 23.5–35.8% for Eu(III) and 21.4–23.3% for Tb(III) establish this type of ligand as a versatile and efficient sensitizer of lanthanide ion emission. Because of the stability of the 3:1 complexes, the emission efficiencies are independent of the counter anion utilized. Emission lifetimes in different solvents also confirm that the 3:1 stoichiometry in solution is stable and effectively prevents the coordination of solvent molecules to the metal ion. These new examples of pyridine-bis(oxazoline)-based complexes substantiate the versatility of this ligand family and its suitability as sensitizer of lanthanide ion luminescence.

Acknowledgment. Grant support through the NSF-CHE 0733458 and PRF #43347-AC3 (A.d.B.D.) as well as NSF-CHE-0936982 (D.T.d.L.) is gratefully acknowledged. Dr. Andrei Poloukhine is acknowledged for help with the initial ligand synthesis.

Supporting Information Available: Figures showing ball-and-stick representations for all complexes, NMR and mass spectra, tables listing the bond lengths, distances and hydrogen bonding distances, as well as absorption, emission and excitation spectra for all species. This material is available free of charge via the Internet at <http://pubs.acs.org>.